Calculations of giant magnetoelectric effects in ferroic composites of rare-earth–iron alloys and ferroelectric polymers

Ce Wen Nan and Ming Li
Department of Materials Science and Engineering, Tsinghua University, Beijing 100084, China

Jin H. Huang
Department of Mechanical Engineering, Feng Chia University, Taichung 407, Taiwan

(Received 31 August 2000; published 19 March 2001)

Coupled magnetic-mechanical-electric effects involving linearly and nonlinearly coupling interactions in ferroic composites are investigated using a Green's function technique. We use the theory to suggest a possible giant magnetoelectric effect in a ferroelectric poly(vinylidene fluoride-trifluorethylene) copolymer filled by giant magnetostrictive rare-earth–iron alloy particles, which is markedly larger than that in the best known magnetoelectric materials. The flexible composite is expected to exhibit large magnetostriction. Our results show how to design such flexible polymer-matrix magnetoelectric composites with better performance and may stimulate further interest in the areas of coupled multifield effects and magnetoelectric materials for practical applications.

DOI: 10.1103/PhysRevB.63.144415 PACS number(s): 75.80.+q, 77.65.–j, 75.50.Bb, 81.05.Zx

I. INTRODUCTION

The magnetoelectric (ME) effect, a coupled magnetic-dielectric effect characterized by the appearance of an electric polarization (ME output) on applying a magnetic field or by the appearance of a magnetization on applying an electric field, was prophetically predicted first by Pierre Curie in 1894 on the basis of symmetry considerations.[1] Until 1960–1961, the linear ME effect was only experimentally observed in an antiferromagnetic Cr_2O_3 crystal.[2] Since then, ME effects have been widely investigated in over ten different crystal families (e.g., yttrium iron garnets, boracites, rare-earth ferrites, and phosphates[3,4]) due to their important applications in solid-state sciences.[5] However, among these single-phase ME materials (which are brittle), particularly strong ME effects, as initially envisioned, have not so far been found, which is the reason that they have not yet found applications in technology.[5] To be technologically viable, ME materials must exhibit high ME coefficients. Important applications include magnetic-electric sensors in radioelectronics, optoelectronics, and microwave electronics and transducers in instrumentation.

In the single-phase ME crystals, the ME effect is intrinsic. However, ferrite/piezoelectric ceramic composites[6–10] such as $CoFe_2O_4/BaTiO_3$ and (Ni-Co-Mn)-ferrite/lead-zirconate-titanate (PZT) composites exhibit extrinsic ME effects, which is known as a ''product property,''[11] resulting from the interaction between the ferrite and piezoelectric ceramic phases, since neither phase is magnetoelectric. That is, when a magnetic field is applied to the composites, the ferrite particles change their shape magnetostrictively, and strain is passed along to the piezoelectric phase, resulting in an electric polarization. The ferroic ceramic composites were considered to exhibit promising larger linear ME effects resulting from the coupled piezoelectric-piezomagnetic interaction.[12–15] However, the ME effect so far observed in such brittle composites is only about ten times or more lower than the predicted value due mainly to inherent preparation problems,[5–10] such as interdiffusion during preparation.

In this article, we consider a novel ferroic composite of a giant magnetostrictive rare-earth–iron alloy [e.g., $SmFe_2$, $TbFe_2$, or $Tb_{1-x}Dy_xFe_2$ (Terfenol-D)] (Ref. 16) and a ferroelectric polymer such as the poly(vinylidene fluoride)-trifluorethylene copolymer [P(VDF-TrFE)],[17] which are, respectively, the best known and most widely used magnetostrictive alloy and ferroelectric polymer. This polymer-matrix composite is mechanically flexible and experimentally fabricated much more easily than the brittle ferrite/piezoelectric ceramic composites. In the flexible Terfenol-D/P(VDF-TrFE) composite, the coupling interaction between magnetostriction (a *nonlinear* magnetomechanical effect) of the Terfenol-D particles and piezoelectricity (a *linear* electromechanical effect) of the P(VDF-TrFE) can also result in an extrinsic ME effect. Here we generalize the Green's function technique[13,18–20] to treat the new type of ME material from the Terfenol-D-filled P(VDF-TrFE)-matrix composite involving both *nonlinearly* and *linearly coupling* interactions. We suggest that the flexible ferroic composite can exhibit a surprisingly large ME effect that is markedly larger than that in the best known ME materials (e.g., Cr_2O_3, phosphates, and ferrite/piezoelectric ceramic composites). In addition, the flexible composite also exhibits large magnetostriction as in the recently developed magnetostrictive composites.[21] This may open up a new promising territory for the applications of inorganic/organic hybrids and composites with magnetic-mechanical-electric coupling interactions.

The rest of this article is organized as follows. In Sec. II, we design a few possible composite Terfenol-D/P(VDF-TrFE) microstructures with a ME effect from a practical point of view. Section III contains the theoretical framework derived by the Green's function technique and the general solution to the ME effect of such a magnetostrictive-piezoelectric composite. For quantitative purposes, the numerical results for the ME effect and effective magnetostriction of the novel Terfenol-D/P(VDF-TrFE) composite are

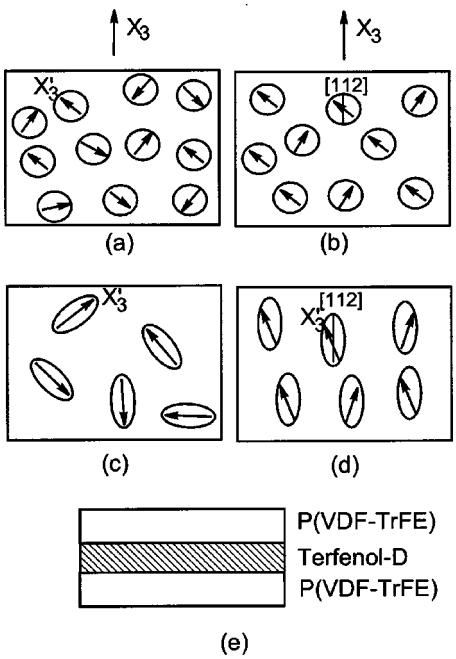

FIG. 1. Schematic illustration of the P(VDF-TrFE) matrix composites filled with (a) randomly and (b) magnetically oriented Terfenol-D spheres (the arrows represent their crystallographic X_3'-axis directions), (c) randomly and (d) magnetically oriented Terfenol-D ellipsoidal particles (in the case of (d) their ellipsoidal symmetric axis growth along the crystallographic [112] or [111]-direction (Refs. 16 and 20)), and (e) the laminated Terfenol-D/P(VDF-TrFE) composite. The polarization direction in P(VDF-TrFE) is parallel to X_3 axis of the composite, along which an external magnetic field $\langle H_3 \rangle$ is applied.

presented for various microstructural features in Sec. IV. The conclusions are summarized in Sec. V.

II. DESIGNING THE MICROSTRUCTURE OF THE TERFENOL-D/P(VDF-TrFE) COMPOSITE

As an external magnetic field is applied to the Terfenol-D/P(VDF-TrFE) composite, the magnetostrictively induced strain of the Terfenol-D phase is passed along to the P(VDF-TrFE) phase, resulting in an electric polarization. This means that the composite has to be electrically insulating, at least along the applied magnetic field direction. Hence, it is required that the low-resistance Terfenol-D particles should be well dispersed in the polymer matrix to keep the composite insulating, since the low-resistance Terfenol-D particle percolation path (especially along the applied magnetic field direction) can make it difficult to polarize the composite and cause the charges developed in the piezoelectric P(VDF-TrFE) phase to leak through this comparatively low-resistance path. According to this, we now design a simple particulate composite with a volume fraction f of equiaxial Terfenol-D microcrystallites[22] randomly or magnetically oriented in the P(VDF-TrFE) matrix without a Terfenol-D particle percolation path through the composite. We also let the P(VDF-TrFE) matrix be poled along the X_3 axis of the composite specimen, as shown in Figs. 1(a) and 1(b). The Terfenol-D particles are not in contact with each other while the polymer is self-connected, thus forming a 0-3 connectivity of phases (in the terminology introduced by Newnham, Skinner, and Cross[23]). The composite has a ∞mm symmetry with ∞ denoting the X_3 axis. Both higher particulate loading (e.g., $f=0.4$) well dispersed in the polymer matrix and magnetically preferred orientation of the Terfenol-D particles can be achieved by current processing techniques[24] such as wet-chemical methods in an orientation magnetic field.[21]

In the piezoelectric ceramic/epoxy composites (e.g., PZT/epoxy) widely investigated[25] [and the magnetostrictive composites (e.g., Terfenol-D/epoxy) recently developed[21]], a technologically important composite with better performance has a 1-3 connectivity of phases. The unidirectional continuous piezoelectric ceramic rods are embedded in the epoxy matrix and aligned parallel to the sample axis X_3. However, a 1-3 composite of Terfenol-D/P(VDF-TrFE) would not have the extrinsic ME effect, since the unidirectionally aligned Terfenol-D rods form low-resistance paths. If prolate-shaped Terfenol-D particles are not in contact with each other but well dispersed in the polymer matrix [Figs. 1(c) and 1(d)], the composite would have the ME effect. However, the geometric shape anisotropy of the Terfenol-D particles leads to low allowable particulate loading to keep the 0-3 connectivity, due to the low percolation threshold.[26] At the other extreme, a multilayer Terfenol-D/P(VDF-TrFE) composite (i.e., with 2-2 connectivity) laminated along the X_3 axis [Fig. 1(e)] should also have the ME effect. Next we quantitatively treat these possible composites with the extrinsic ME effect.

III. GENERAL FRAMEWORK

Consider the perfectly bonded Terfenol-D/P(VDF-TrFE) composites, as shown in Fig. 1. For Terfenol-D with cubic symmetry, the magnetomechanical interaction is a *nonlinear coupling* effect, namely,

$$\sigma = \mathbf{c}\varepsilon - \chi^T \mathbf{H}\mathbf{H},$$

$$\mathbf{B} = \mu \mathbf{H} + \chi \varepsilon \mathbf{H}, \tag{1}$$

where σ, ε, $\mathbf{B}$, and $\mathbf{H}$ are the stress tensor, strain tensor, magnetic induction (or flux density), and magnetic field, respectively; χ is the magnetostrictive coefficient (χ^T being the transpose of χ); $\mathbf{c}$ and μ are, respectively, the stiffness at constant field and permeability tensor at constant strain. For Terfenol-D, these three coefficient tensors (χ, $\mathbf{c}$, and μ) are more or less dependent on the magnetic and stress fields.[16,27] Equation (1) can simply be rewritten as[20]

$$\sigma = \mathbf{c}(\varepsilon - \varepsilon^{ms}),$$

$$\mathbf{B} = \mu(\varepsilon, \mathbf{H})\mathbf{H}, \tag{2}$$

where the permeability μ depends on ε and $\mathbf{H}$, and ε^{ms} is the magnetostrictively induced strain of Terfenol-D. The local magnetostrictive strains, ε_{ij}^{ms}, along the crystallographic axes of a Terfenol-D microcrystallite are related to the magnetic field dependent magnetostriction constants, λ_{100} and λ_{111}, of the cubic microcrystallite. These constants are defined as the

change in normal strain in the [100] and [111] crystallographic directions resulting from the complete rotation of a fully random magnetization state into the [100] and [111] directions, respectively.[16] The strains can be expressed as

$$\varepsilon_{ij}^{ms}=\begin{cases}\dfrac{3}{2}\lambda_{100}\left(\beta_{3i}^2-\dfrac{1}{3}\right) & \text{for } i=j\\ \dfrac{3}{2}\beta_{3i}\beta_{3j}\lambda_{111} & \text{for } i\neq j,\end{cases}\tag{3}$$

where (β_{ij}) is the matrix transforming the local crystallographic axes X_j' to the material axes X_i, in which an external magnetic field $\langle H_3\rangle$ is applied along X_3 axis of the materials specimen (Fig. 1), namely, $X_i=\beta_{ij}X_j'$.[20] Thus ε_{ij}^{ms} is nonlinearly dependent on **H**.

On the other hand, for the piezoelectric P(VDF-TrFE) phase, the electromechanical interaction is a *linear coupling* effect, namely,

$$\sigma=\mathbf{c}\varepsilon-\mathbf{e}^T\mathbf{E},\qquad \mathbf{D}=\mathbf{e}\varepsilon+\kappa\mathbf{E},\tag{4}$$

where **D** and **E** are the electric displacement and field tensors, respectively; **e** is the piezoelectric coefficient tensor ($\mathbf{e}^T$ being the transpose of **e**); κ is the dielectric constant tensor at constant strain. The response of their composite involving the *nonlinear* and *linear coupling* effects can be described by the combination of Eqs. (2) and (4), as

$$\sigma=\mathbf{c}\varepsilon-\mathbf{e}^T\mathbf{E}-\mathbf{c}\varepsilon^{ms},\qquad \mathbf{D}=\mathbf{e}\varepsilon+\kappa\mathbf{E}+\alpha\mathbf{H},\qquad \mathbf{B}=\mu(\varepsilon,\mathbf{E},\mathbf{H})\mathbf{H},\tag{5}$$

where the permeability μ depends on ε and electric and magnetic fields; α is the ME coefficient. For the composite, all these tensors are local quantities depending on the spatial position **x**. The effective properties of the composite can be defined in terms of the averaged fields, namely,

$$\langle\sigma\rangle=\mathbf{c}^*\langle\varepsilon\rangle-\mathbf{e}^{T*}\langle\mathbf{E}\rangle-\mathbf{c}^*\varepsilon^{ms*},\qquad \langle\mathbf{D}\rangle=\mathbf{e}^*\langle\varepsilon\rangle+\kappa^*\langle\mathbf{E}\rangle+\alpha^*\langle\mathbf{H}\rangle,\qquad \langle\mathbf{B}\rangle=\mu^*(\langle\varepsilon\rangle,\langle\mathbf{E}\rangle,\langle\mathbf{H}\rangle)\langle\mathbf{H}\rangle,\tag{6}$$

where angular brackets denote the microstructural average and quantities with asterisks represent those of the composite. Therefore, the problem of evaluating the effective response of the material essentially consists of the determination of the field variables within it under certain specified boundary conditions, followed by the performance of the averages.

Because of spatial variations in the constitutive behavior in the composite with position, the local constitutive coefficients can be written as a variation about a mean value, e.g.,

$$\mathbf{c}(\mathbf{x})=\mathbf{c}^0+\mathbf{c}'(\mathbf{x}),\quad \kappa(\mathbf{x})=\kappa^0+\kappa'(\mathbf{x}),\quad \mu(\mathbf{x})=\mu^0+\mu'(\mathbf{x}),\tag{7}$$

where the first terms (denoted by superscript 0) represent the constitutive constants of a homogeneous reference medium and the second terms are the spatial fluctuations of the first.

Now let the composite be subjected on its external surface S to homogeneous mechanical-electric-magnetic boundary conditions, i.e.,

$$u_i(S)=\varepsilon_{ij}^0x_j=u_i^0,\quad \phi(S)=-E_i^0x_i=\phi^0,\quad \psi(S)=-H_i^0x_i=\psi^0,\tag{8}$$

where u_i, ϕ, and ψ, respectively, denote the elastic displacement, electric potentials and magnetic potential. Consider a state of static equilibrium in the absence of body forces and free electric charges so that

$$\sigma_{ij,j}(\mathbf{x})=0,\quad D_{i,i}(\mathbf{x})=0,\quad B_{i,i}(\mathbf{x})=0,\tag{9}$$

where the commas in the subscripts denote partial differentiation with respect to x_j [e.g., $\sigma_{ij,j}(\mathbf{x})=\partial\sigma_{ij}(\mathbf{x})/\partial x_j=0$]. These are nonlinearly coupling equilibrium equations.

Further, by solving the equilibrium equations (9) under the boundary conditions (8) in terms of the Green's function technique,[13,18–20] the local fields within the composite can be obtained as

$$\varepsilon=\varepsilon^0+\mathbf{G}^u(\mathbf{c}-\mathbf{c}^0)\varepsilon-\mathbf{G}^u\mathbf{e}^T\mathbf{E}-\mathbf{G}^u\mathbf{c}^{ms},\qquad \mathbf{E}=\mathbf{E}^0+\mathbf{G}^\phi\mathbf{e}\varepsilon+\mathbf{G}^\phi(\kappa-\kappa^0)\mathbf{E}+\mathbf{G}^\phi\alpha\mathbf{H},\qquad \mathbf{H}=\mathbf{H}^0+\mathbf{G}^\psi(\mu-\mu^0)\mathbf{H},\tag{10}$$

where $\mathbf{G}^u$, $\mathbf{G}^\phi$, and $\mathbf{G}^\psi$ are the modified displacement, electric potential, and magnetic potential Green's functions for the homogeneous medium.[18] Iterative solutions of Eq. (10) yield

$$\varepsilon=\mathbf{T}^{66}\varepsilon^0-\mathbf{T}^{63}\mathbf{E}^0-\mathbf{T}^{66}\mathbf{G}^u\mathbf{c}\varepsilon^{ms}-\mathbf{T}^{63}\mathbf{G}^\phi\alpha\mathbf{T}^{33m}\mathbf{H}^0,\qquad \mathbf{E}=\mathbf{T}^{36}\varepsilon^0+\mathbf{T}^{33e}\mathbf{E}^0-\mathbf{T}^{36}\mathbf{G}^u\mathbf{c}\varepsilon^{ms}+\mathbf{T}^{33e}\mathbf{G}^\phi\alpha\mathbf{T}^{33m}\mathbf{H}^0,\qquad \mathbf{H}=\mathbf{T}^{33m}\mathbf{H}^0,\tag{11}$$

with

$$\mathbf{T}^{66}=\{\mathbf{I}-\mathbf{G}^u(\mathbf{c}-\mathbf{c}^0)+\mathbf{G}^u\mathbf{e}^T[\mathbf{I}-\mathbf{G}^\phi(\kappa-\kappa^0)^{-1}\mathbf{G}^\phi\mathbf{e}\}^{-1},$$

$$\mathbf{T}^{33e}=\{\mathbf{I}-\mathbf{G}^\phi(\kappa-\kappa^0)+\mathbf{G}^\phi\mathbf{e}[\mathbf{I}-\mathbf{G}^u(\mathbf{c}-\mathbf{c}^0)]^{-1}\mathbf{G}^u\mathbf{e}^T\}^{-1},$$

$$\mathbf{T}^{63}=\mathbf{T}^{66}\mathbf{G}^u\mathbf{e}^T[\mathbf{I}-\mathbf{G}^\phi(\kappa-\kappa^0)]^{-1},\qquad \mathbf{T}^{36}=\mathbf{T}^{33e}\mathbf{G}^\phi\mathbf{e}[\mathbf{I}-\mathbf{G}^u(\mathbf{c}-\mathbf{c}^0)]^{-1},\qquad \mathbf{T}^{33m}=[\mathbf{I}-\mathbf{G}^\psi(\mu-\mu^0)]^{-1},\tag{12}$$

where **I** is the unit tensor. Substitution of Eq. (11) into Eq. (5) directly gives explicit solutions for the local field σ, **D**, and **B**, also as a function of ε^0, $\mathbf{E}^0$, and $\mathbf{H}^0$.

By averaging these solutions for local field quantities and eliminating ε^0, $\mathbf{E}^0$, and $\mathbf{H}^0$ from them, and further by considering that **e** ($\mathbf{e}^T$)=0 for the Terfenol-D phase, $\varepsilon^{ms}=0$ for

the P(VDF-TrFE) phase, and $\alpha=0$ for both phases, we obtain the general solutions to overall effective properties of the composite

$$\mathbf{c}^*=\langle \mathbf{cT}^{66}-\mathbf{e}^T\mathbf{T}^{36}\rangle\mathbf{A}+\langle \mathbf{cT}^{63}+\mathbf{e}^T\mathbf{T}^{33e}\rangle\mathbf{B}, \tag{13}$$

$$\mathbf{e}^{T*}=\langle(\mathbf{c}-\mathbf{c}^*)\mathbf{T}^{63}+\mathbf{e}^T\mathbf{T}^{33e}\rangle\langle\mathbf{T}^{33e}\rangle^{-1}, \tag{14}$$

$$\kappa^*=\langle(\mathbf{e}^*-\mathbf{e})\mathbf{T}^{63}+\kappa\mathbf{T}^{33e}\rangle\langle\mathbf{T}^{33e}\rangle^{-1}, \tag{15}$$

$$\mu^*=\langle\mu\mathbf{T}^{33m}\rangle\langle\mathbf{T}^{33m}\rangle^{-1}, \tag{16}$$

$$\varepsilon^{ms*}=(\mathbf{c}^*)^{-1}\langle[(\mathbf{c}-\mathbf{c}^*)\mathbf{T}^{66}\mathbf{G}^u+\mathbf{I}]\mathbf{c}\varepsilon^{ms}\rangle, \tag{17}$$

$$\alpha^*\langle\mathbf{H}\rangle=\mathbf{e}^*\langle\mathbf{T}^{66}\mathbf{G}^u\mathbf{c}\varepsilon^{ms}\rangle, \tag{18}$$

with $\mathbf{A}=[\langle\mathbf{T}^{66}\rangle+\langle\mathbf{T}^{63}\rangle\langle\mathbf{T}^{33e}\rangle^{-1}\langle\mathbf{T}^{36}\rangle]^{-1}$ and $\mathbf{B}=\langle\mathbf{T}^{33e}\rangle^{-1}\langle\mathbf{T}^{36}\rangle\mathbf{A}$. These results are quite general and independent of the models assumed for the topology of the phases in the composite. These complicated, coupled expressions lack closed form solutions, but their convenient matrix formulations are particularly suited for easily numerical calculations of the overall effective properties. Equations (13)–(16) recover the expressions previously used for these effective coefficient tensors,[18] and Eq. (17) is similar to the previous expression for the effective magnetostrictively induced strain[20] but contains the effect of piezoelectricity of the P(VDF-TrFE) phase through $\mathbf{c}^*$. Equation (18) is the desired formula for the composite ME coefficient resulting from the coupling interactions between the *nonlinear magnetostrictive* and *linear piezoelectric* effects and clearly demonstrates that the ME coefficient of such a composite does not disappear though neither phase is magnetoelectric.

Further, Eqs. (18) and (17) can be rewritten as

$$\alpha^*\langle\mathbf{H}\rangle=f\mathbf{e}^*\langle[\mathbf{I}-\mathbf{G}^u(\mathbf{c}-\mathbf{c}^0)]^{-1}\mathbf{G}^u\mathbf{c}\varepsilon^{ms}\rangle_{orient}, \tag{19}$$

$$\varepsilon^{ms*}=f(\mathbf{c}^*)^{-1}\langle[(\mathbf{c}-\mathbf{c}^*)[\mathbf{I}-\mathbf{G}^u(\mathbf{c}-\mathbf{c}^0)]^{-1}\times\mathbf{G}^u+\mathbf{I}]\mathbf{c}\varepsilon^{ms}\rangle_{orient}, \tag{20}$$

where $\langle\,\rangle_{orient}$ denotes averaging over all possible orientations of the Terfenol-D microcrystallites in the composite and $\mathbf{c}$ is the stiffness tensor of Terfenol-D particles. From Eq. (19), the primary ME output voltage $\overline{\mathbf{E}}$ induced by the magnetostrictive-piezoelectric coupling interaction is given as

$$\overline{\mathbf{E}}=\kappa^{*-1}\alpha^*\langle\mathbf{H}\rangle=\alpha_E^*\langle\mathbf{H}\rangle \tag{21}$$

$$=f\mathbf{h}^*\langle[\mathbf{I}-\mathbf{G}^u(\mathbf{c}-\mathbf{c}^0)]^{-1}\mathbf{G}^u\mathbf{c}\varepsilon^{ms}\rangle_{orient}, \tag{22}$$

where $\mathbf{h}^*$ $(=\kappa^{*-1}\mathbf{e}^*)$ is the effective piezoelectric stress coefficient tensor and α_E^* is the ME voltage coefficient or ME sensitivity tensor. Equation (22) shows that a strong ME response of the composites could be achieved with the large magnetostrictively induced strain, high piezoelectric stress coefficients, and the perfect coupling between the phases (i.e., transferring elastic strains without appreciable losses).

Depending on the choice made for the properties (e.g., $\mathbf{c}^0$, κ^0, and μ^0) of the homogeneous reference medium, two different approximate schemes pertain and can be easily obtained from the general solutions above. One is that the polymer matrix phase is taken as the homogeneous reference medium, e.g., $\mathbf{c}^0=\mathbf{c}^m$, $\kappa^0=\kappa^m$ and $\mu^0=\mu^m$. This choice leads to a simple non-self-consistent approximate (NSCA) scheme[18,19] of the theory. In essence it is generally valid for matrix-based composites with a particulate microstructure, such as those shown in Figs. 1(a) and 1(b). Another is to consider the constituent phases embedded in an effective medium that corresponds to the overall composite itself but with the moduli that must be determined self-consistently, and thus a generalized self-consistent effective medium approximation (SCA) is realized. Phenomenologically, this SCA corresponds to the Bruggeman-Landauer self-consistent approximation for transport problem or the Kröner-Hill-Budiansky self-consistent approximation for elastic problem.[19] The good quantitative agreement of previous results of the Green's function-based theory and experiment for piezoelectric and magnetostrictive composites[18–20] has demonstrated the predictive power of the theoretical approach. Next we mainly predict the extrinsic ME response of the Terfenol-D/P(VDF-TrFE) composites (Fig. 1), since the Terfenol-D is the best known and most widely used giant magnetostrictive alloy[16] and the P(VDF-TrFE) polymer has larger piezoelectric stress coefficient (comparable to that for a piezoelectric ceramic).[17] In addition, the polymer-matrix composites can be easily processed and conformed to complicated shapes and surfaces, and the coupling between two phases may be enhanced by the improved displacement transfer capability of the flexible polymer matrix itself.

IV. ME EFFECT OF TERFENOL-D/P(VDF-TrFE) COMPOSITES AND DISCUSSION

On applying an external magnetic field $\langle H_3\rangle$ alone along the symmetric X_3 axis of the composite specimen (Fig. 1), the ME output voltage $\overline{E_3}$ developed across the specimen along the X_3 direction is

$$\overline{E_3}=\alpha_{33}^*\langle H_3\rangle/\kappa_{33}^*=\alpha_{E33}\langle H_3\rangle \tag{23}$$

from Eq. (21), where α_{E33} is the ME sensitivity along the $\langle H_3\rangle$ direction, which is the figure of merit used to assess the performance of a ME material for a magnetic device. The effective engineering magnetostriction,[16] $\overline{\lambda_s}=\frac{2}{3}(\varepsilon_{33}^{ms*}-\varepsilon_{11}^{ms*})$, can directly be obtained from Eq. (20).[20] Now for quantitative purposes, numerical calculations are performed for the Terfenol-D/P(VDF-TrFE) composite. The properties of these phases used for calculations are given in Table I. We consider three different orientations of Terfenol-D microcrystallites in the P(VDF-TrFE) matrix, i.e., random orientation, partly magnetic [112] orientation, and optimally magnetic [111] orientation (i.e., all [112] or [111] crystallographic directions of the microcrystallites being parallel to the X_3 axis).[16,20]

For illustrative purposes, Fig. 2 shows the numerical results in the high-magnetic-field saturation in the whole vol-

TABLE I. Properties of Terfenol-D and P(VDF-TrFE) and PZT-5A used in the present numerical calculations.

Properties	Terfenol-D [a]	P(VDF-TrFE) [b]	PZT-5A [c]
c_{11} (GPa)	82	4.84	121
c_{12} (GPa)	40	2.72	75.4
c_{13} (GPa)	40	2.22	75.2
c_{33} (GPa)	82	4.63	111
c_{44} (GPa)	38	0.526	21.1
ϵ_{33}/ϵ_0	6	8	830
μ_{33}/μ_0	5	1	1
e_{31} (C/m^2)	0	0.0043	-5.4
e_{33} (C/m^2)	0	-0.11	15.8
e_{15} (C/m^2)	0	-0.015	12.3
h_{33} (10^9 V/m)	0	-1.55	2.15
λ_{111} (ppm)	1700	0	0
λ_{100} (ppm)	100	0	0

[a]Terfenol-D exhibits a cubic symmetry, and its properties are taken by referring to Refs. 16 and 20. $\mu_{33}/\mu_0=5$ at zero magnetic field and decreases almost linearly with increasing magnetic field to 1.8 in the saturation; the magnetic field dependence of λ_{111} and λ_{100} is shown in the right part of Fig. 4(b).

[b]For convenience, the symmetry properties of P(VDF-TrFE) are considered to belong to the point group *6mm* due to only slight differences between its e_{31} and e_{32}, e_{15} and e_{24}, c_{11} and c_{22}, c_{13} and c_{23}, c_{44} and c_{55}, and ϵ_{11} and ϵ_{22}; we take these property values mainly by referring to Ref. 28.

[c]Reference 29.

ume fraction range. As in the ferrite/piezoceramic composites,[12,13] the ME sensitivity of the composite increases from zero to the maxima with increasing f and then approach zero at $f=1$. The NSCA and SCA predict different maximum ME sensitivities at different volume fractions (e.g., at $f\approx 0.85$ and 0.55 for NSCA and SCA, respectively) and different results at high concentration, but they give very close results in the volume fraction range of $f<0.4$ of interest, within which both approximations are considered to be valid and the polymer-matrix composite as shown in Figs. 1(a) and 1(b) can be easily fabricated. The results of the two approximation schemes being almost the same at $f<0.4$ mean also that the theoretical predictions in this volume fraction range of interest are reasonable. (We will use the simpler NSCA scheme of theory in the following calculations.) As shown previously for other magnetostrictive composites,[20] the effective saturation magnetostriction of the composite monotonically increases with the volume fraction f (not presented here). As with the effective magnetostriction,[20] the ME sensitivity of the composite is larger in the magnetically preferred orientation cases of the Terfenol-D particles than in the random orientation case. Figure 2(b) shows dependence of the ME sensitivity on the effective magnetostriction. It can be seen that α_{E33} is proportional to $\overline{\lambda_s}^n$ with $n=1-2$ at the range $f<0.4$ of interest. Of particular interest is that a surprisingly large ME effect is obtained in the composite. The α_{E33} values at $f=0.3$ are 2.2, 2.9, and 3.8 V/A, respectively, for the random, [112], and

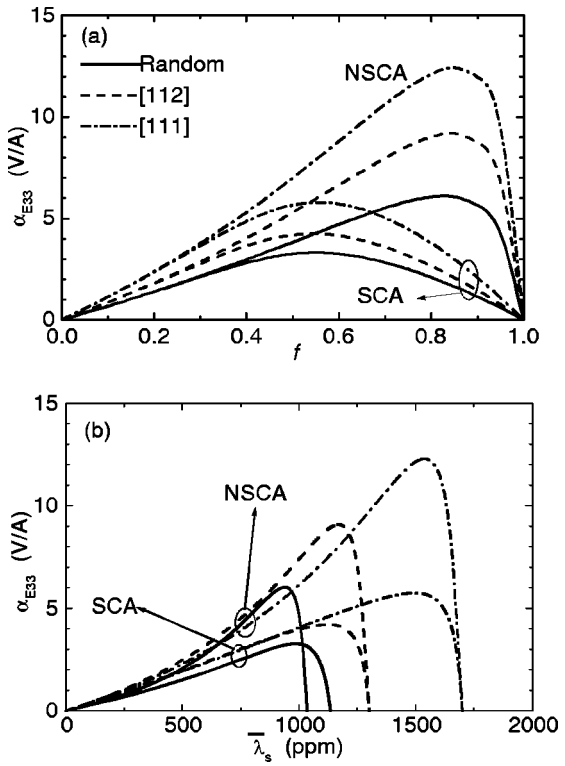

FIG. 2. ME sensitivity α_{E33} and engineering magnetostriction $\overline{\lambda_s}$ of the P(VDF-TrFE) matrix composite [Figs. 1(a) and 1(b)] filled with random, partly magnetic [112], and optimally magnetic [111] oriented of Terfenol-D particles, in the whole volume fraction range at the high magnetic field saturation predicted by using the NSCA and SCA schemes of theory.

[111] orientation of Terfenol-D particles, which are markedly larger than the maximum α_{E33} values for the best known ME materials at room temperature, i.e., $\alpha_{E33}^{\max}\sim 0.038$ V/A (at above 200 kA/m) for the antiferromagnetic Cr_2O_3 crystal[5] and $\alpha_{E33}^{\max}\sim 0.15$ V/A (at 72 kA/m) measured for the ferrite/PZT ceramic composite.[8,9] In the meantime, this flexible composite can exhibit large saturation magnetostriction, e.g., $\overline{\lambda_s}=460$ ppm for the randomly oriented Terfenol-D particle ($f=0.3$) case.

For comparison, we hypothesize an idealized PZT ceramic matrix composite consisting of perfectly bonded Terfenol-D particles without interdiffusion between Terfenol-D particles and PZT matrix. Figure 3 illustrates the comparison between the results for the flexible Terfenol-D/P(VDF-TrFE) composite and brittle Terfenol-D/PZT ceramic composite (the properties of the PZT-5A used for calculations are also listed in Table I). Although the predicted ME coefficient α_{33}^* [Fig. 3(b)] of the brittle Terfenol-D/PZT ceramic composite is roughly 80–100 times larger than that of the flexible Terfenol-D/P(VDF-TrFE) composite due to lower piezoelectric coefficients e_{ij} (see Table I) of the P(VDF-TrFE) than PZT, the ME sensitivity α_{E33} and the effective magnetostriction [Fig. 3(a)] of the P(VDF-TrFE)-matrix composite are larger than those of the brittle PZT ceramic matrix composite. This is due to the improved displacement transfer capability of the flexible polymer matrix,

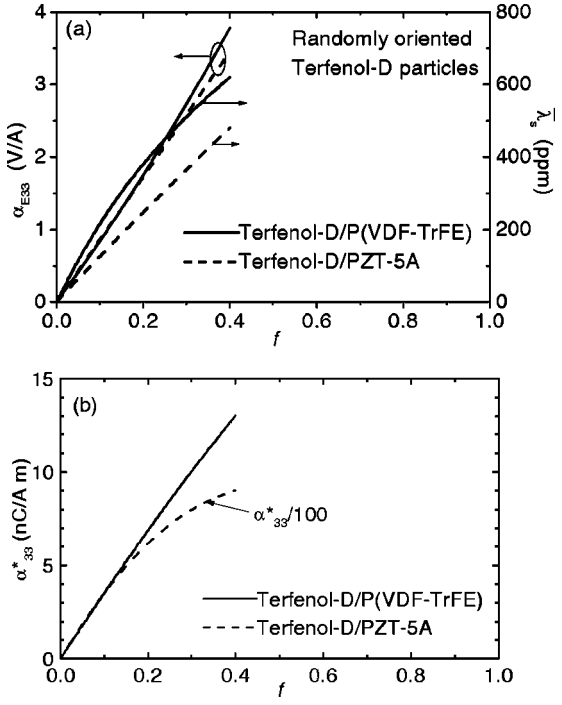

FIG. 3. Comparison of the predicted ME effect and engineering magnetostriction $\overline{\lambda_s}$ of the flexible P(VDF-TrFE)-matrix composite and brittle PZT ceramic matrix composite (the sign of its α^*_{33} and α_{E33} being negative) filled with randomly oriented Terfenol-D particles [Fig. 1(a)].

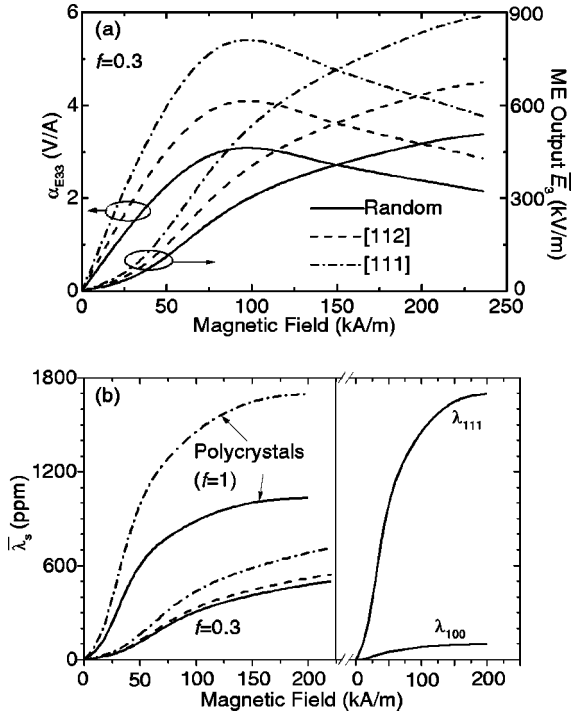

FIG. 4. (a) ME response and (b) engineering magnetostriction $\overline{\lambda_s}$ of the P(VDF-TrFE) matrix composite [Figs. 1(a) and 1(b)] filled with three different orientations of Terfenol-D particles at $f=0.3$ as a function of the magnetic field. The calculated engineering magnetostriction of Terfenol-D polycrystals ($f=1$) and the magnetic-field-dependent magnetostriction constants (λ_{111} and λ_{100}) used for the present numerical calculations are also reported in (b) for comparison.

which leads to higher magnetostriction of the flexible composites and a piezoelectric stress coefficient h_{33} (see Table I) of P(VDF-TrFE) comparable to that of PZT.

Due to the nonlinear dependence of the magnetostriction of Terfenol-D on the applied magnetic field,[16] the effective magnetostriction of the composite nonlinearly increases with the magnetic field as in the Terfenol-D polycrystal [Fig. 4(b)]. The ME sensitivity α_{E33} nonmonotonically depends on $\langle H_3 \rangle$ with a maximum value [Fig. 4(a)] appearing at the magnetic field where the effective magnetostriction begins to approach its saturation. At high magnetic fields the magnetostriction becomes saturated, producing a nearly constant electric field in P(VDF-TrFE), thereby decreasing α_{E33} with increasing $\langle H_3 \rangle$. The maximum $\alpha_{E33}^{\max}$ values (at $\langle H_3 \rangle = 90$ kA/m) are 3.1, 4.1, and 5.4 V/A, respectively, for the random, [112], and [111] orientation of Terfenol-D particles ($f=0.3$), which are also markedly larger than those for the best-known ME materials at room temperature. The ME voltage $\overline{E_3}$ monotonically increases with the magnetic field [Fig. 4(a)] as does the effective magnetostriction [Fig. 4(b)]. Hence, the flexible composite would be tuned to a desired sensitivity to detect either small or very large magnetic fields.

Figure 5 more clearly shows orientation effects by considering two different orientation cases: (1) a uniform orientation distribution between $\theta=0$ and θ_{cutoff} of the local X_3' axes with respect to the sample X_3 axis, and (2) an identical orientation at some angle θ of all local X_3' axes with respect to the sample X_3 axis. The ME sensitivity α_{E33} exhibits the same dependence on particle orientation as the effective magnetostriction. Obviously, only when [111] directions of all microcrystallites are identically aligned parallel to the sample X_3 axis, i.e., $\theta=55°$ (or 145°) for the identical orientation case do the magnetostriction $\overline{\lambda_s}$ and thus the ME sensitivity α_{E33} reach a maximum, and they decrease with a deviation of θ from 55°. When all local X_3' axes are aligned parallel to the applied magnetic field (i.e., $\theta=0$ or π), $\overline{\lambda_s} \rightarrow \sim \varepsilon_{33}^{ms*} \rightarrow \sim \lambda_{100}$,[20] and thus this leads to a low ME effect.

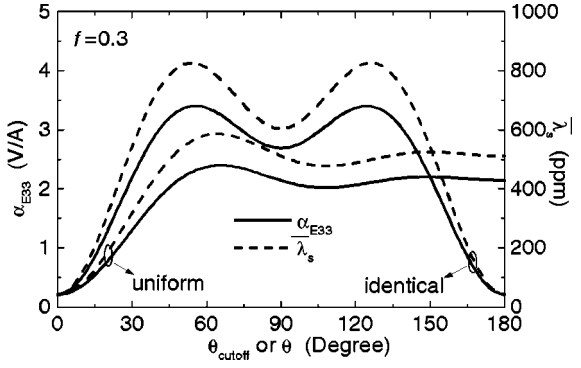

FIG. 5. Effect of the two types of particle orientation distributions (uniform and identical orientations) on the ME sensitivity of the 30 vol % Terfenol-D/P(VDF-TrFE) composite [Fig. 1(a)].

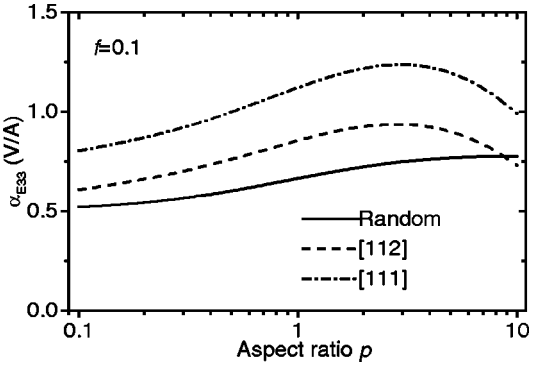

FIG. 6. Effect of the aspect ratio of Terfenol-D particles on the ME sensitivity of the 10 vol % Terfenol-D/P(VDF-TrFE) composite [Figs. 1(c) and 1(d)].

As shown, the orientation distribution of the particles also affects the ME sensitivity α_{E33}. In the case of a uniform orientation distribution between $\theta=0$ and θ_{cutoff}, α_{E33} (as $\overline{\lambda_s}$) reaches a maximum at about $\theta_{cutoff}=65°$. The uniform distribution shifts the angle of the maximum α_{E33} from the standard 55° to 65° due to interactions between various oriented particles. Similarly, α_{E33} in this uniform distribution case increases with θ_{cutoff} as $\theta_{cutoff}<65°$, and decreases as $\theta_{cutoff}>65°$; but $\theta_{cutoff}>90°$, α_{E33} somewhat fluctuates about the ME sensitivity for the completely random case.

For the microstructure shown in Figs. 1(c) and 1(d), the shape anisotropy of the Terfenol-D particles limits low allowable particulate loading in the 0-3 connectivity case due to the low percolation threshold.[26] For illustration, Fig. 6 reports the calculated results from the oblate-shaped particles (aspect ratio $p<1$) to prolate-shaped particles ($p>1$) at $f=0.1$. α_{E33} is not very sensitive to the aspect ratio in the case of low f and small deviation of p from 1. Figure 7 shows the predictions for the 2-2 type laminated Terfenol-D/P(VDF-TrFE) composite [Fig. 1(e)]. It also demonstrates the large ME effect of the laminated composite.

In the calculations above (Figs. 2–7), we have used the materials parameters [see Table I and the right part of Fig. 4(b)] similar to those of the Terfenol-D single crystal itself

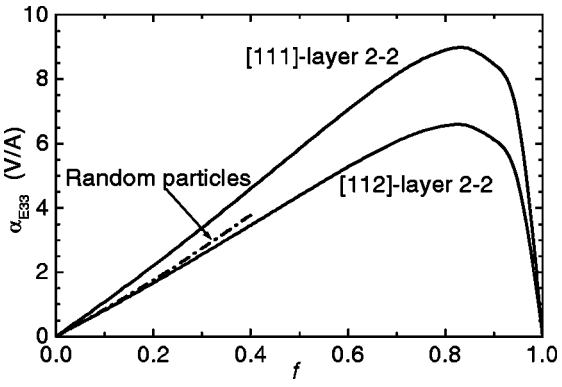

FIG. 7. The ME sensitivity of the 2-2 type laminated Terfenol-D/P(VDF-TrFE) composite [Fig. 1(e)] for [111] and [112] growth directions of Terfenol-D layers with an aspect ratio of 0.1.

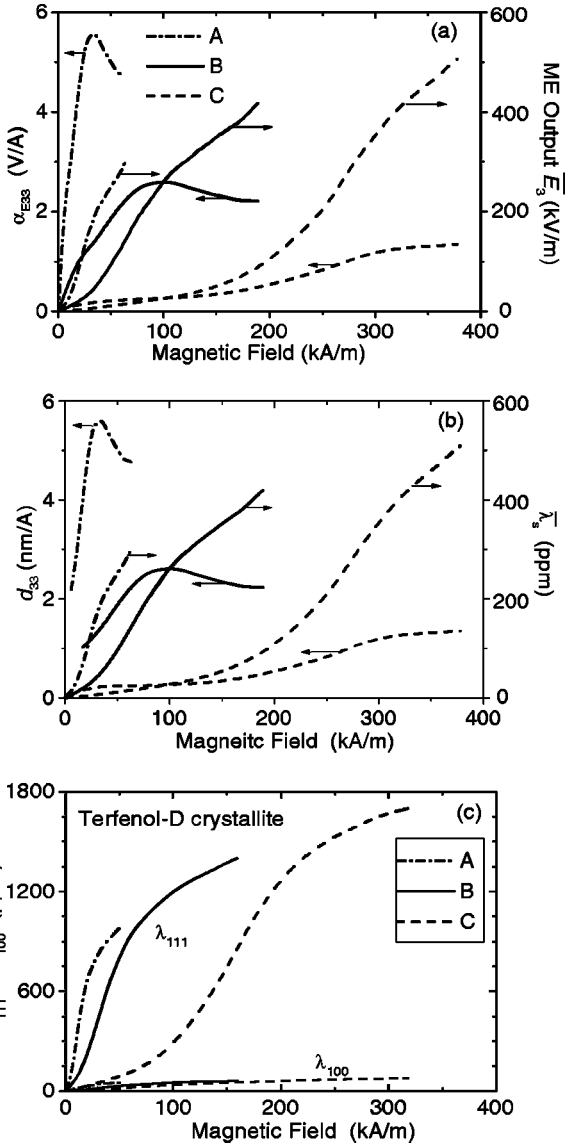

FIG. 8. (a) ME response and (b) engineering magnetostriction $\overline{\lambda_s}$ and secant piezomagnetic coefficient $d_{33}=\overline{\lambda_s}/\langle H_3\rangle$ of the P(VDF-TrFE) matrix composite [Fig. 1(a)] filled with randomly oriented Terfenol-D particles at $f=0.3$ as a function of the magnetic field, calculated by assuming three different behaviors [A, B, and C curves shown in (c)] of the magnetic-field-dependent magnetostriction constants (λ_{111} and λ_{100}) for Terfenol-D.

for the Terfenol-D microcrystallites in the composite. This is, in general, reasonable for the large grain size of Terfenol-D in the composites, as shown in previous calculations for magnetostrictive composites.[20] However, the materials parameters of the Terfenol-D microcrystallites in the composites might be different from the Terfenol-D single crystal itself. The Terfenol-D in the composites is under constraint by the surrounding polymer matrix, i.e., is somewhat under a prestress state. In the absence of any intrinsic materials parameters for the Terfenol-D microcrystallites in the composites, we assume three different dependences of the magnetostriction constants λ_{111} and λ_{100} [see Fig. 8(c)] on the magnetic field to illustrate the influence of the magneto-

strictive behavior of the Terfenol-D microcrystallites on the ME response of the composites. For convenience, we still use those values in Table I for c_{ij}, ε_{33}, and μ_{33} of the Terfenol-D. The calculated ME response and effective engineering magnetostriction $\overline{\lambda}_s$ and ''secant piezomagnetic coefficient'' d_{33} $(=\overline{\lambda}_s/\langle H_3\rangle)$ of the composites are shown in Figs. 8(a) and 8(b), respectively. Comparison of Fig. 8 demonstrates that the ME response of the composites is closely related to the magnetostrictive behavior of Terfenol-D. As already shown above [Figs. 2(b) and 4], the ME output $\overline{E}_{33}$ is proportional to $\overline{\lambda}_s$, i.e., $\overline{E}_{33}\propto\overline{\lambda}_s$, and thus α_{E33} is proportional to d_{33}, i.e., $\alpha_{E33}\propto d_{33}$. As expected, large magnetostrictive coefficients lead to large ME sensitivity of the composites.

Finally we would like to address that our model hypothesizes a perfectly bonded Terfenol-D particle/polymer interface, which ensures the perfect coupling between these two phases (i.e., transferring elastic strains without appreciable losses) to obtain exceptional control of the predictability of the ME composites. Any imperfect interfaces will more or less decrease the displacement transfer capability, thereby leading to a decrease in the ME response of the composites. Especially when the particle sizes are small, say nanoscale sized, the effect of the imperfect interface will be more pronounced due to a large amount of interfaces in the composites. However, as with the technologically important piezoelectric ceramic/epoxy and magnetostrictive composites extensively investigated,[21,25] the quantitative correlation between the coupling behavior for real composites and their interface imperfection remains to be explored.

V. CONCLUSIONS

The effective coupling properties of the flexible Terfenol-D/P(VDF-TrFE) composite have been expressed in a convenient matrix formulation by using the successful Green's function technique. Although the Terfenol-D and P(VDF-TrFE) phases exhibit no magnetoelectric effect, our results suggest that the Terfenol-D-particle-filled P(VDF-TrFE)-matrix composite and laminated Terfenol-D/P(VDF-TrFE) composite may be a type of giant ME material. The large ME response of the Terfenol-D/P(VDF-TrFE) composites is due to the giant magnetostriction of Terfenol-D and large piezoelectric stress coefficients of the P(VDF-TrFE) polymer, as well as the coupling between two phases enhanced by the improved displacement transfer capability of the flexible polymer matrix itself. The ferroic composite can be mechanically flexible and fabricated easily in a variety of forms such as large flexible thin sheets, extruded bars, and molded shapes. Like the technologically important piezoelectric and magnetostrictive composites extensively investigated,[21,25] the Terfenol-D/P(VDF-TrFE) composite could be an important material for magnetic-electric devices.[30] This may open up new promising territory for the applications of inorganic/organic hybrids and composites with magnetic-mechanical-electric coupling interactions.

ACKNOWLEDGMENTS

This work was supported by the NSF of China (Grant No. 59825102), the Ministry of Sciences and Technology of China (Grant No. G2000067108), Tsinghua Foundation (Grant No. JZ2000007), and Taiwan NSC (NSC 89-2212-E-035-014).

[1] *Magnetoelectric Interaction Phenomena in Crystals*, edited by A. J. Freeman and H. Schmid (Gordon and Breach, London, 1975).
[2] V. J. Folen, G. T. Rado, and E. W. Stalder, Phys. Rev. Lett. **6**, 607 (1961); G. T. Rado and V. J. Folen, *ibid.* **7**, 310 (1961); D. Astrov, Zh. Éksp. Teor. Fiz. [Sov. Phys. JETP **13**, 729 (1961)].
[3] *Proceedings of the 2nd International Conference on Magnetoelectric Interaction Phenomena in Crystals MEIPIC-2* [Ferroelectrics **161 & 162** (1994)].
[4] *Proceedings of the 3rd International Conference on Magnetoelectric Interaction Phenomena in Crystals MEIPIC-3* [Ferroelectrics **204** (1997)].
[5] H. Schmid, Ferroelectrics **161**, 1 (1994).
[6] A. M. J. G. van Run, D. R. Terrell, and J. H. Scholing, J. Mater. Sci. **9**, 1710 (1974).
[7] G. Harshe, J. P. Dougherty, and R. E. Newnham, Int. J. Appl. Electromagn. Mater. **4**, 145 (1993).
[8] S. Lopatin, I. Lopatin, and I. Lisnevskaya, Ferroelectrics **162**, 63 (1994).
[9] M. I. Bichurin, I. A. Kornev, V. M. Petrov, and I. Lisnevskaya, Ferroelectrics **204**, 289 (1997).
[10] K. K. Patankar, S. A. Patil, K. V. Sivakumar, R. P. Mahajan, Y. D. Kolekar, and M. B. Kothale, Mater. Chem. Phys. **65**, 97 (2000).
[11] J. van Suchtelen, Philips Res. Rep. **27**, 28 (1972).
[12] I. Getman, Ferroelectrics **162**, 45 (1994).
[13] C. W. Nan, Phys. Rev. B **50**, 6082 (1994).
[14] Y. Benveniste, Phys. Rev. B **51**, 16 424 (1995); J. Li and M. L. Dunn, Philos. Mag. A **77**, 1341 (1998).
[15] J. H. Huang, Phys. Rev. B **58**, 12 (1998); T. L. Wu and J. H. Huang, Int. J. Solids Struct. **37**, 2981 (2000).
[16] A. E. Clark, in *Ferromagnetic Materials*, edited by E. M. Wohlfarth (North-Holland, Amsterdam, 1980), Vol. 1, p. 531.
[17] *Ferroelectric Polymers*, edited by H. S. Nalwa (Marcel Dekker, New York, 1995).
[18] C. W. Nan and F.-S. Jin, Phys. Rev. B **48**, 8578 (1993); C. W. Nan, J. Appl. Phys. **76**, 1155 (1994).
[19] C. W. Nan and D. R. Clarke, J. Am. Ceram. Soc. **80**, 1333 (1997).
[20] C. W. Nan, Appl. Phys. Lett. **72**, 2897 (1998); C. W. Nan and G. J. Weng, Phys. Rev. B **60**, 6723 (1999).
[21] See, for example, L. Sandlund, M. Fahlander, T. Cedell, A. E. Clark, J. B. Restorff, and M. Wun-Fogle, J. Appl. Phys. **75**, 5656 (1994); M. Anjanappa and Y. Wu, Smart Mater. Struct. **6**, 393 (1997); J. Hudson, S. C. Busbridge, and L. R. Piercy, Sens. Actuators **81**, 294 (2000).
[22] In the particulate composites designed, the particle sizes of Terfenol-D are considered to be large such as about 100 μm.

For large particle sizes, the particle size effect is very weak. See, for example, J. Hudson, S. Busbridge, and A. R. Piercy, Ferroelectrics **228**, 283 (1999). However, as the particle size of Terfenol-D decreases, the particle size effect will become marked due mainly to the increase in interface content and the changes in properties of small Terfenol-D crystallites themselves.

[23] R. E. Newnham, D. P. Skinner, and L. E. Cross, Mater. Res. Bull. **13**, 525 (1978).

[24] *Organic/Inorganic Hybrid Materials*, edited by R. M. Laine, C. Sanchez, E. Giannelis, and C. J. Brinker, MRS Symposia Proceedings No. 519 (Materials Research Society, Warrendale, 1998).

[25] A. Safari, Mater. Res. Innov. **2**, 263 (1999); J. A. Chilton, GEC Rev. **6**, 156 (1999).

[26] C. W. Nan, Prog. Mater. Sci. **37**, 1 (1993).

[27] M. B. Moffett, A. E. Clark, M. Wun-Fogle, J. Linberg, J. P. Teter, and E. A. McLaughlin, J. Acoust. Soc. Am. **89**, 1448 (1991).

[28] H. Wang, Q. M. Zhang, L. E. Cross, and A. O. Sykes, J. Appl. Phys. **74**, 3394 (1993).

[29] *Landolt-Bornstein: Numerical Data and Functional Relationships in Science and Technology* (Springer-Verlag, Berlin, 1990), Group 3, Vol. 24.

[30] L. P. M. Bracke and R. G. van Vlite, Int. J. Electron. **51**, 255 (1981); J. L. Prieto, C. Aroca, E. Lopez, M. C. Sanchez, and P. Sanchez, J. Magn. Magn. Mater. **215/216**, 756 (2000).